

Preparation and Anticorrosive Properties of Hybrid Coatings Based on Epoxy-Silica Hybrid Materials

Kuan-Yeh Huang,¹ Chang-Jian Weng,¹ Su-Yin Lin,¹ Yuan-Hsiang Yu,² Jui-Ming Yeh¹

¹Department of Chemistry, Center for Nanotechnology at CYCU, Chung-Yuan Christian University, Chung Li, Taiwan 32023, Republic of China

²Department of Electronic and Electro-Optical Engineering, Lan Yang Institute of Technology, I Lan, Taiwan 261, Republic of China

Received 29 February 2008; accepted 4 September 2008

DOI 10.1002/app.29302

Published online 12 February 2009 in Wiley InterScience (www.interscience.wiley.com).

ABSTRACT: A series of sol-gel derived organic-inorganic hybrid coatings consisting of organic epoxy resin and inorganic silica were successfully synthesized through sol-gel approach by using 3-glycidoxypropyl-trimethoxysilane as coupling agent. Transparent organic-inorganic hybrid sol-gel coatings with different contents of silica were always achieved. The hybrid sol-gel coatings with low silica loading on cold-rolled steel coupons were found much superior improvement in anticorrosion efficiently. The as-synthesized hybrid sol-gel materials

were characterized by Fourier-transformation infrared spectroscopy, ²⁹Si-nuclear magnetic resonance spectroscopy and transmission electron microscopy. Effects of the material composition of epoxy resins along with hybrid materials on the thermal stability, Viscoelasticity properties and surface morphology were also studied, respectively. © 2009 Wiley Periodicals, Inc. *J Appl Polym Sci* 112: 1933–1942, 2009

Key words: epoxy resin; sol-gel; corrosion protection

INTRODUCTION

Most metals corrode through charge transfer reactions in an ambient environment, which may cause deterioration occurring at the metal surface.¹ This metallic corrosion causes considerable waste of natural resources.² In the earlier stage, chromium containing compounds were often used as anticorrosion coating materials. Recently, increased research activities shifted to find alternative materials based on the environmental and health concerns.

Protective organic coatings are typically employed as a primer to protect steel surface from corrosion. However, poor adhesion of coating materials to the steel can cause not only delamination of the coating material but also corrosion of the steel substrate beneath the coating material. Therefore, adhesion strength of coating materials chemisorbed on various metallic substrates is a critical issue to develop alternative novel advanced corrosion protection coatings. The effectiveness of the organic coating relied primarily on the interfacial adhesion strength between metallic surface and polymeric coatings. Thus, proper corrosion inhibitors are usually required to

extend the service life of steel. Therefore, various silane coupling agents had been used as a primer for increasing the corrosion protection effect of pure polymer coatings due to the enhancement of interfacial adhesion strength between the metallic surface and polymeric coatings.^{3–8}

The sol-gel process has been used usually to prepare creamer coatings and to protect the metal surface from corrosion.^{9–11} During the sol-gel process, metal alkoxides as sol-gel precursor produced a condensed film as barrier layer on the metal substrate through the hydrolysis and condensation reaction. In the past decade, several reports have been dedicated to the corrosion protection of metals, by sol-gel derived organic-inorganic hybrids.^{12–14} Organofunctional alkoxysilane are frequently used as sol-gel precursors for the adhesion promoter application between two different phases such as polymer coatings and metallic surface. Four-functional alkoxysilane, i.e., tetraethyl orthosilicate (TEOS) or tetramethyl orthosilicate (TMOS) was commonly used and reported to have better corrosion protection efficiency when compared with pure polymer coating. TEOS has also been applied as a binder in preparing coating formulation for preparing zinc-rich primer.¹⁵ Holmes-Farley and Yanyo reported that TEOS in conjunction with aminosilane can be used to prevent corrosion on aluminum substrates.¹⁶

Lately, research results on the preparation of the epoxy resin based organic-inorganic hybrids have

Correspondence to: J.-M. Yeh (juiming@cycu.edu.tw).

Contract grant sponsor: NSC; contract grant number: 92-2113-M-033-004.

been reported. For example, Matejka and coworkers^{17,18} have attained epoxy-silica hybrids by different synthesis procedures. In the one-step procedure, all reaction components are mixed and reacted to form hybrids. In the two-step procedures, TEOS is first prehydrolyzed in the presence of the catalyst toluenesulfonic acid. Subsequently, the hydrolyzed TEOS is mixed with the diglycidyl ether of bisphenol A and D-2000 hardener to form hybrids. Other experiments^{19,20} based on a functional group, such as the amine group, coupling agent have been developed to study the morphology of hybrid materials and the properties. However, they had seldom been mentioned for practical applications.

Recently, Yeh et al.²¹ reported that the evaluation of corrosion protection effect of neat epoxy resin-clay nanocomposite and the PMMA-SiO₂ (thermal plastic) hybrid coatings²² by a series of electrochemical corrosion measurements. We found that it may enhance the anticorrosion properties efficiently.

In this article, we successfully synthesized the epoxy-SiO₂ (thermosetting plastic) hybrid coatings and presented the effective incorporation of the corrosion-protection enhancing factors (i.e., adhesion promoter) into epoxy resin through sol-gel approach and evaluated their corrosion protection effect on the surface of cold-rolled steel (CRS) coupons. We envisioned that the enhancement of corrosion protection effect of the hybrid sol-gel coatings may be due to the increase of adhesion strength and surface hydrophobicity of hybrid sol-gel coatings on CRS coupons relative to pure epoxy resin as evidenced by Fourier-transformation infrared and reflection absorption spectroscopy (FTIR-RAS) and contact angle test. The as-prepared samples were further identified by a series of electrochemical measurements such as corrosion potential (E_{corr}), polarization resistance (R_p), corrosion current (I_{corr}), and electrochemical impedance spectroscopy studies in 5 wt % NaCl electrolyte.

EXPERIMENT SECTION

Materials and sample preparation

TMOS (Aldrich, USA) was purified by distillation before use. An epoxy resin, diglycidyl ether of bisphenol A (DGEBA, Epikote 828 EL, Fluka, Germany) with the epoxy equivalent weight of 180 g/mol and 3-glycidyl-oxypopyltrimethoxysilane (GLYMO 98%, Aldrich). Poly(oxypropylene)triamine (Jeffamine T403, Huntsman Corp.) was used as a curing agent for epoxy and as a basic catalyst of GLYMO hydrolysis. Acetone (Acros) and hydrochloric acid (Riedel-De Haen, 37%) were used as received without further purification.

Thermal ring-opening polymerization of epoxy resin

A typical procedure to prepare the epoxy resin was given as follows: 5 g of DGEBA, 1.751 g of T403, and 5 g acetone were put into beaker. After magnetically stirring at room temperature for 10 min, this as-prepared homogeneously viscous colorless solution was subsequently cast onto CRS coupons or glass substrate under vacuum, then following the heating program at 80°C for 10 min, 100°C for 10 min, 140°C for 30 min, and 150°C for 30 min. The transparent neat epoxy resin coating material was obtained and named epoxy.

Synthesis of P(DGEBA-co-GLYMO) copolymer

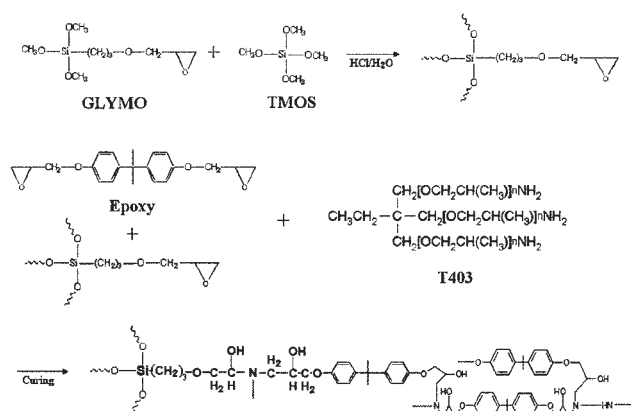
The conventional procedure employed to prepare the P(DGEBA-co-GLYMO) epoxy copolymer materials (DG). 1.0 g of GYLMO and 5 g of DGEBA were dissolved in 5 g of acetone. 1.751 g of T403 as curing agent was added with further stirring at room temperature for 10 min. The resultant mixture was degassed and drop wisely cast onto a CRS followed by curing under vacuum at 80°C for 10 min, 100°C for 10 min, 140°C for 30 min, and 150°C for 30 min.

Preparation of epoxy-silica hybrid coating materials

Epoxy-silica hybrid coating materials were given as follows: 0.23 g of TMOS, 0.04 g of HCl (2N), 5 g of acetone, and 1 g of GLYMO were all put into beaker and stirred in ambient condition for 1 h. 5 g of DGEBA, 1.751 g of T403, and 5 g acetone were then put into the solution (DG03). The resultant homogeneous solution was stirred at room temperature for 30 min, the obtained clear gel solution was subsequently coated on the CRS coupons, further thermal treatment were performed in an oven under 80°C for 10 min, 100°C for 10 min, 140°C for 30 min, and 150°C for 30 min to complete the sol-gel reactions of as-prepared hybrid sol-gel coating until the sample weight became essentially constant. The typical flow-chart for the preparation of epoxy-silica hybrid sol-gel materials was given as Scheme 1.

Instrumentation

FTIR and FTIR-RAS were recorded by using a JASCO FTIR 460 Plus spectrometer. The samples of epoxy-SiO₂ hybrid materials for transmission electron microscopy (TEM) study were microtomed with Reichert-Jung Ultracut-E into 60–90 nm-thick slices. Subsequently, one layer of carbon about 10-nm thick was deposited on these slices on mesh 100 copper nets for TEM observations on a JEOL-200FX with an acceleration voltage of 120 kV. Electrochemical



Scheme 1 Flow chart for the preparation of epoxy-silica hybrid sol-gel materials with GLYMO as coupling agent.

measurements of corrosion potential, polarization resistance, and corrosion current, on sample-coated CRS coupons were performed on VoltaLab 21 potentiostat/galvanostat in a standard corrosion cell equipped with two graphite rod counter electrodes and a saturated calomel electrode as well as the working electrode. Thermogravimetric analyses (TGA) were performed under nitrogen flow using TA Q50 at the heating rate 10°C/min from 30 to 750°C. Differential scanning calorimetry (DSC) was performed under nitrogen flow using TA Q10 at the heating rate 10°C/min from 30 to 150°C. Dynamic mechanical analysis (DMA) was performed on a TA Q800. The programmed heating rate is 3°C/min and a fixed frequency of 20 Hz was used and the heating range is performed from 30 to 110°C. The surface hardness testing of the bulky epoxy-silica hybrid sol-gel materials were tested by TECLOCK, GS-706N (Type D). The contact angle of epoxy-silica hybrid sol-gel coatings was measured by First Ten Angstroms (FTA) 125. Scanning electron microscope (SEM) was obtained with a Hitachi S-2300 SEM. Atomic force microscope (AFM) analysis was used to probe the surface morphology of the coated hybrid sol-gel films by using an AFM of Digital Instrument, Inc., model DI 5000.

Preparation of coatings and electrochemical measurements^{23–25}

The clear gel solutions of epoxy-silica hybrid mixture with different silica content were cast drop wisely onto the CRS coupons (1.0 × 1.0 cm²), followed by drying in air for 24 h at 40°C to give coatings of about 120 μm in thickness measured through a digimatic micrometer (Mitutoyo). The coating ability of epoxy-silica hybrid materials on CRS was found to be similar to that of neat epoxy resin. The coated and uncoated coupons were then mounted on the working electrode so that only the coated

side of the coupon was in direct contact with the electrolyte. The edges of the coupons were sealed with super fast epoxy cement[®]. All the electrochemical measurements of corrosion potential, polarization resistance, and corrosion current were performed on a VoltaLab model 21 potentiostat/galvanostat and repeated at least three times. The electrolyte was NaCl (5 wt %) aqueous solution. Polarization resistance (R_p in Ω/cm²) was measured by sweeping the applied potential from 20 mV below to 20 mV above the E_{corr} at a scan rate of 500 mV/min and by recording the corresponding current change. The R_p value was obtained from the slope of the potential-current plot. Tafel plots were obtained by the scanning potential from 250 mV below to 250 mV above the E_{corr} at a scan rate of 500 mV/min. Corrosion current (I_{corr}) was determined by superimposing a straight line along the linear portion of the cathodic or anodic curve and extrapolating it through E_{corr} . The corrosion rate (R_{corr} , in milli-inches per year, MPY) was calculated from the following equation: where EW is the equivalent weight (in g/equiv), A is the area (in cm²), and d is the density (in g/cm³).

$$R_{\text{corr}}(\text{MPY}) = [0.13i_{\text{corr}}(\text{E.W.})]/[A.d]$$

RESULTS AND DISCUSSIONS

To synthesize epoxy-silica hybrid sol-gel materials, the HCl-catalyzed sol-gel reactions of coupling agent (GLYMO) and TMOS were prepared as a precursor materials, followed by performing the conventional ring opening reactions of DGEBA with Jaffamine T403 as curing agent. The composition of the copolymer (DG) and the hybrid materials which added 3, 5, 10 wt % of TMOS were with respect to materials content as named in Table I.

Characterizations

Representative FTIR absorption spectra of neat epoxy and hybrid materials were illustrated in Figure 1. The characteristic vibration bands of DGEBA were shown at 1609 cm⁻¹, 1508 cm⁻¹ (C—C skeletal stretching), 1036 cm⁻¹ (aromatic deformation), and 913 cm⁻¹ (epoxide ring) for epoxy. The first step involves the reactions between epoxide ring of epoxy resin and primary amino groups of T403 that was confirmed by the disappearance of characteristic epoxide band at ~ 913 cm⁻¹ and appearance of hydroxyl band at 3400 cm⁻¹,²⁶ shown in Figure 1(a). The gel reaction of the hybrid composites can be monitored with FTIR as shown in Figures 1(b) and 2–4. The absorption band around 1100 cm⁻¹ which is associated with the Si—O—Si linkages can also be observed in all hybrid composites.²⁷ The FTIR peaks

TABLE I
Relations of the Composition of the Epoxy, Epoxy-Silica Hybrid Sol-Gel Coatings with the E_{corr} , R_p , I_{corr} , and R_{corr} as well as with the Adhesion of the Coatings onto CRS as Estimated from Electrochemical Methods

Sample code	Feed composition		Electrochemical corrosion measurement ^a					Thickness ^b (μm)	P_{EF} (%)
	P (Epoxy-co-GLYMO) (wt %)	TMOS (wt %)	E_{corr} (mV)	I_{corr} ($\mu\text{A}/\text{cm}^2$)	R_p ($\text{K}\Omega \text{cm}^2$)	R_{corr} (MPY)			
Bare	0	0	-716	49.5	1.53	0.58	0	0	
Epoxy	0	0	-698	37.9	1.95	0.44	121	2.52	
DG	100	0	-682	24.8	2.62	0.29	124	4.75	
DG03	97	3	-645	15.0	4.64	0.18	118	9.91	
DG05	95	5	-609	10.5	6.31	0.12	120	14.94	
DG10	90	10	-589	7.1	10.00	0.08	117	17.74	

^a Saturated calomel electrode (SCE) was employed as reference electrode.

^b As measured by a digimatic micrometer.

of 1036 cm^{-1} of epoxy and hybrid materials were corresponded to aromatic deformation and the epoxy monomer was further reacting with the secondary hydroxyl groups of the high-molecular weight epoxy resin to form an ether linking at 1233 cm^{-1} ($\text{C}-\text{O}-\text{C}$)²⁸

Figure 2 displays the solid-state ^{29}Si -NMR spectrum of as-prepared epoxy-silica hybrid materials. In condensed siloxane species for TMOS, silicon atoms

through mono-, di-, tri-, and tetra-substituted siloxane bonds are designated as Q^1 , Q^2 , Q^3 , and Q^4 , respectively. For 3-glycidyloxypropyltrimethoxysilane, mono-, di-, tri-substituted siloxane bonds are designated as T^1 , T^2 , T^3 , respectively. In this study, the chemical shifts of Q^4 and T^3 are -109 and -65 ppm, respectively, and conform to the literature value.²⁹ The results revealed that Q^4 and T^3 are the major microstructures in the network structure of the hybrid composites.

Figure 3 shows the TEM photographs of DG10 (scale bar 500 nm), which was found to show some dispersed silica particles (ca. 100–500 nm) in epoxy matrix, which might be associated with the simultaneous processing of sol-gel reactions for the trialkoxysilyl functional groups in the copolymers and tetraalkoxysilyl functional groups of TMOS.

Potentiodynamic measurements

Corrosion protection performance of the sample-coated CRS coupons was evaluated by the studies of electrochemical corrosion measurements such as the corrosion potential (E_{corr}), polarization resistance (R_p), corrosion current (I_{corr}), and corrosion rate (R_{corr}), as listed in Table I. Tafel plots obtained from electrochemical corrosion measurements for (a), (b), (c), (d), and (e) for uncoated, epoxy-coated, DG-

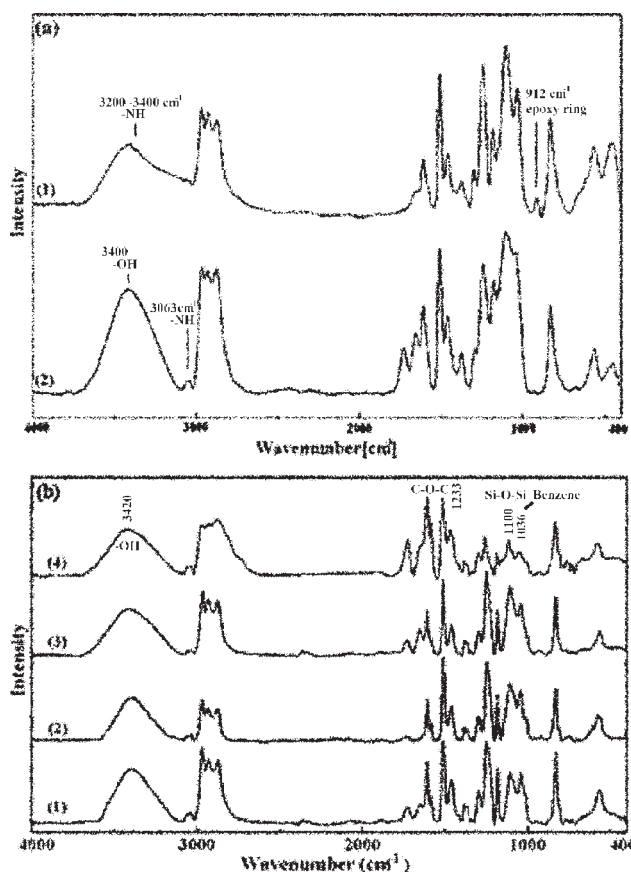


Figure 1 Representative FTIR spectra of (a) neat epoxy resin polymerization: (1) before ring-opening and (2) after ring-opening; (b) as-prepared materials in the form of coating: (1) epoxy, (2) DG, (3) DG05, and (4) DG10.

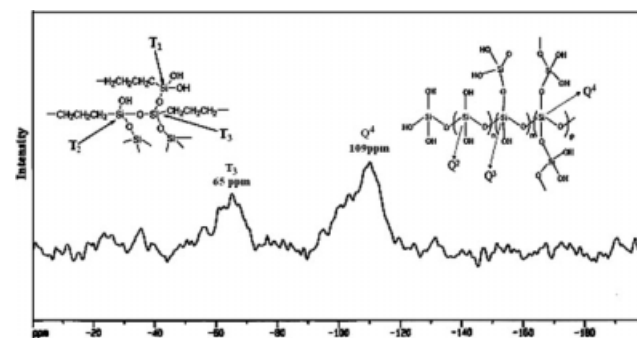


Figure 2 Solid-state ^{29}Si -NMR spectrum of as-prepared epoxy-silica hybrid materials.

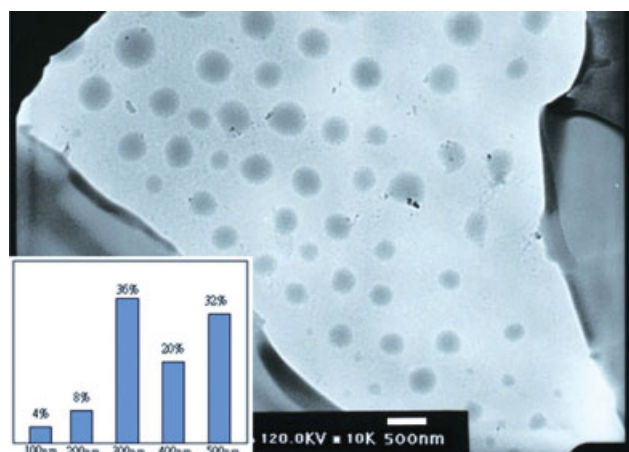


Figure 3 TEM photographs of DG10 hybrid materials ($\times 10k$). [Color figure can be viewed in the online issue, which is available at www.interscience.wiley.com.]

coated, DG03-coated, DG05-coated CRS electrode, respectively, at 500 mV/min are shown in Figure 4.

The coated CRS coupons showed a higher E_{corr} value than the uncoated CRS. However, it exhibited a lower E_{corr} value than the specimen-coated with hybrid materials. For example, the DG-coated CRS had a high corrosion potential of about -682 mV at 30 min. Even after 5 h measurement, the potential remained at about -680 mV. Such an E_{corr} value implied that the DG-coated CRS exhibited improved corrosion protection performance toward the electrochemical corrosion compared with the pure epoxy.

The polarization resistances, R_p , were evaluated from the Tafel plots, according to the Stearn-Geary equation,³⁰

$$R_p = b_a b_c / 2.303(b_a + b_c) I_{\text{corr}}$$

Here, I_{corr} is the corrosion current determined by an intersection of the linear portions of the anodic and cathodic curves, and b_a and b_c are anodic and cathodic Tafel slopes ($\Delta E/\Delta \log I$), respectively. The protection efficiency ($P_{\text{EF}}\%$) values were estimated using the following equation³¹:

$$P_{\text{EF}}\% = \frac{100[R_p^{-1}(\text{uncoated}) - R_p^{-1}(\text{coated})]}{R_p^{-1}(\text{coated})}$$

These corrosion parameters calculated from Tafel plots for several composite materials were summarized in Table I. Moreover, electrochemical corrosion current values of hybrid materials as coatings on CRS were found to decrease gradually with further increase of silica loading. Furthermore, it should be noted that the R_{corr} and I_{corr} of DG5 is smaller than that of DG, indicating that coatings with SiO_2 par-

ticles may exhibit excellent corrosion protection performance. On the other hands, from the viewpoints of protection efficiency, we found that DG10 coating exhibited a larger value of $P_{\text{EF}}\%$ than that of epoxy-coated electrode, as shown in Table I. The incorporation of SiO_2 particles into epoxy led to an enhancing protection efficiency of ~ 7 times ($17.74/2.52$) drastically. It is interesting that we also found the incorporation of SiO_2 particles into epoxy matrix showing an increase in protection efficiency as the SiO_2 particles contents increasing. This conclusion implied that, in this study, we envisioned that the enhanced corrosion protection effect of epoxy-silica hybrid sol-gel coatings on metallic surface relative to neat epoxy might probably be resulted from the enhancement of adhesion strength and surface hydrophobicity of hybrid coatings on CRS coupons relative to that of epoxy coating. All the data were repeated at least three times to ensure reproducibility. This can be further evidence by the studies of FTIR-RAS and contact angle measurement in the following section.

FTIR-RAS studies

We envisioned that the enhancement of adhesion strength of epoxy-silica hybrid coatings on CRS coupons compared to neat epoxy may probably be attributed to the formation of covalent bond ($\text{Fe}-\text{O}-\text{Si}$) between the CRS interface and hybrid coatings on the CRS surface, which can be further confirmed by the spectroscopy studies. Compared with pure epoxy [Fig. 5(a)], the curve fitting spectrum of FTIR-RAS studies for the as-prepared hybrid coating DG10 [Fig. 5(b)] showing two novel peaks appeared at around 959 cm^{-1} (due to the $\text{Si}-\text{OH}$) and 995 cm^{-1} (designated to the formation of covalent bond $\text{Fe}-\text{O}-\text{Si}$), respectively. The band at 995 cm^{-1} corresponded to $\text{Fe}-\text{O}-\text{Si}$, which indicated that the covalent bond was made between CRS and

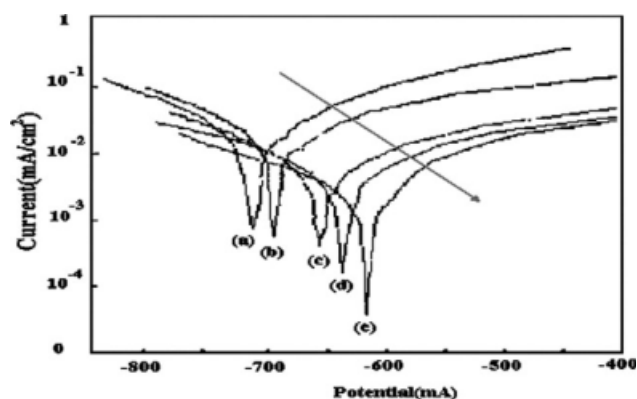


Figure 4 Tafel plots for (a) uncoated, (b) epoxy-coated, (c) DG-coated, (d) DG03-coated, and (e) DG05-coated CRS measured in 5 wt % NaCl aqueous solution.

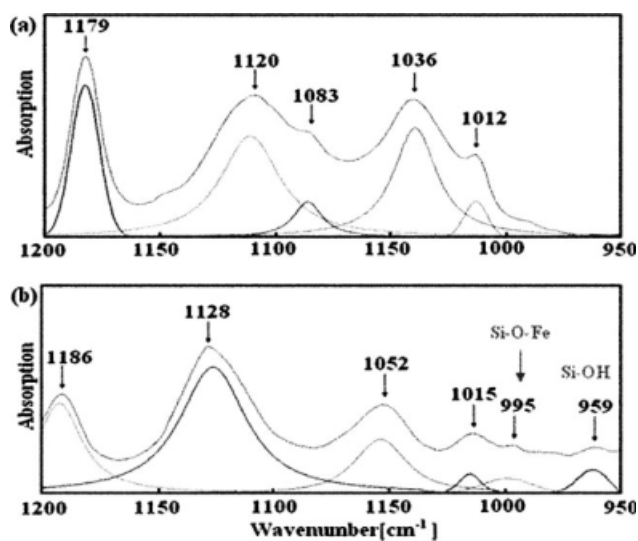


Figure 5 The curve fit spectrum of FTIR-RAS of (a) epoxy and (b) DG10.

hybrid coating on the CRS surface. Jang and Kim had reported the formation of (Fe—O—Si) bond at 995 cm^{-1} between the interface of epoxy-silane coupling agent and steel based on the FTIR-RAS.

Thermal analysis

TGA thermograms of weight loss as a function of temperature for epoxy and a series of hybrid sol-gel materials were studied, as measured under an air atmosphere. The concluding TGA results were illustrated and summarized in Figure 6 and Table II. Evidently, the thermal decomposition temperature (5% weight loss) of copolymer (e.g., T_d of DG = 332.5°C) shifted toward the higher temperature range than that of epoxy ($T_d = 329.0^\circ\text{C}$). As the TMOS content was increased to 10%, T_d of hybrid sol-gel materials was upward to 362.1°C , which confirmed the further enhancement of thermal stability of epoxy by the incorporation of larger loaded inorganic silica particles.

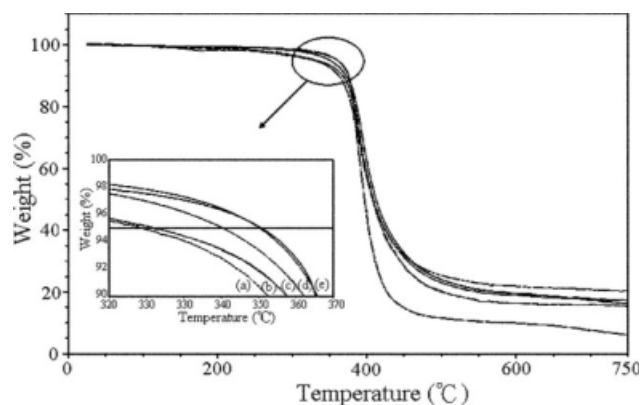


Figure 6 TGA curves for (a) epoxy, (b) DG, (c) DG03, (d) DG05, and (e) DG10.

Furthermore, the glass transition temperature is the important factor associated with the segmental mobility of polymer. The DSC results of epoxy and a series of hybrid sol-gel materials were also shown in Table II. For example, epoxy exhibited an endotherm at 56.40°C , corresponding to the T_g . As the TMOS content was increased to 10%, T_g of hybrid sol-gel materials was upward to 75.08°C , which indicating the incorporation of silica particles into polymer matrix may inhibit the segmental motions of polymer chains.

Viscoelasticity measurement

The thermo-mechanical properties of composite materials were also investigated through the performing of DMA tests using a tension mode. Typically, two different moduli, that is, elastic or storage modulus and an imaginary (loss) modulus were identified in the curves of DMA thermograms. The ratio of loss modulus to storage modulus, which typically reached a maximum point, was called $\tan \delta$ and employed as glass transition temperature (T_g) of as-preparation polymer. The DMA measured results based on the storage modulus

TABLE II
Thermal Properties, Mechanical Properties, and Surface Roughness Properties of the Epoxy, Epoxy-SiO₂ Hybrid Sol-Gel Materials in the Form of Coating as Measured by DSC, TGA, DMA, and AFM

Sample code	Thermal properties			Mechanical properties ^a		Surface roughness ^b	
	T_g^c ($^\circ\text{C}$)	T_d^d ($^\circ\text{C}$)	Char yield ^c (wt %)	Storage modulus (MPa)	$\tan \delta$ ($^\circ\text{C}$)	R_a (nm)	R_q (nm)
Epoxy	56.40	329.0	3.1	1247	56.8	0.207	0.260
DG	62.83	332.5	14.2	1335	62.3	0.182	0.230
DG03	67.87	349.4	15.3	1574	68.6	0.179	0.228
DG05	72.61	360.4	15.8	1626	72.1	0.179	0.226
DG10	75.08	362.1	18.8	1741	74.4	0.180	0.228

^a As measured by TGA. T_d was weight loss the temperature value that 5 wt %.

^b As measured by DSC.

^c As measured by DMA.

^d As measured by AFM. R_a and R_q are the average and root mean square roughness, respectively.

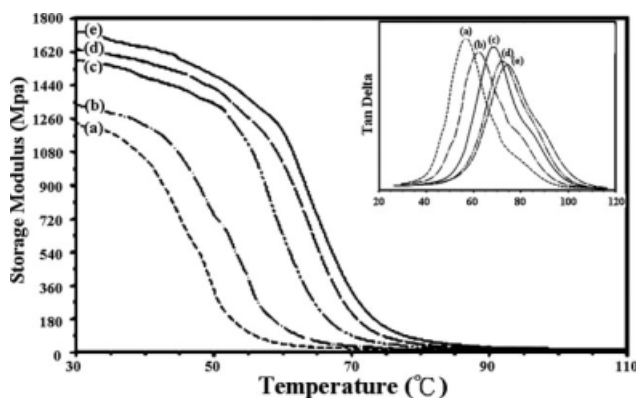


Figure 7 DMA curves for (a) epoxy, (b) DG, (c) DG03, (d) DG05, and (e) DG10: storage modulus and $\tan \delta$ of baked bulky hybrid.

studies of neat epoxy and a series of hybrid sol-gel materials were given in Figure 7 and summarized in Table II. For example, the storage modulus of hybrid sol-gel material, DG03, was remarkably increased by 26% from 1247 MPa of neat epoxy to 1574 of DG03 at around 30°C. Moreover, it is also found that a further increase in SiO₂ concentration resulted in an enhanced mechanical strength of hybrid sol-gel materials (e.g., storage modulus of DG10 = 1741 MPa).

Moreover, the $\tan \delta$ of DG series hybrid materials was higher than the neat epoxy. The maximum value of $\tan \delta$ (neat epoxy) was notice around 56.8°C, this value was smaller than all hybrid materials listed in Table II and Figure 7. As the thermal treatment or silica content increased, the $\tan \delta$ of hybrid materials were increased obviously. By the incorporation of silica into the polymer matrix in form the nanoparticles, it was expected that the rigidity of the composite materials would be significantly improved though extensive interfacial interaction between the organic and inorganic phases. As the motions of the polymer chain were hindered by silica, the $\tan \delta$ was increased considerably. This is probably because of the Brownian motion of network chains.²⁸ The results were consistent with our previous DSC studies. In this study, we found that the value of T_g obtained from the DSC and DMA were very similar. To distinguish this difference between conventional DSC and DMA measurements, the DSC usually has relatively poor sensitivity but DMA is very sensitive to T_g .³²

The hybrid materials exhibit a significant increase in storage modulus with the increase in the silica content during the entire monitoring temperature range, which maybe probably associated with the higher SiO₂ loading in polymer matrix leading to a higher interfacial area between the organic and inorganic phases.

Hardness test

Mechanical strength can be evaluated by the surface hardness of materials. The hardness tests were all performed on the surface of as-prepared samples (i.e., neat copolymer and a series of hybrid sol-gel materials), as demonstrated in Figure 8. For example, copolymer (e.g., DG) exhibited a hardness value of 69 mNt (Shore D), which was obviously higher than that of epoxy (i.e., 64 mNt). On the other hand, the increase of silica concentration in hybrid sol-gel materials corresponded to an increase of surface hardness. For example, the hardness of hybrid sol-gel material at high silica concentration (e.g., DG10, hardness = 80 mNt) was found to be higher than that of hybrid sol-gel materials at low silica concentration (e.g., DG03, hardness = 74 mNt). In conclusion, the incorporation of silica particles into polymer matrix may effectively increase the mechanical strength of polymer based on the surface hardness tests on the as-prepared materials.

Contact-angle (wettability) measurement of coating surface

As exemplified in Figure 9, the water contact angle increased with the increase in silica content in the hybrid sol-gel materials, reflecting to an increase of hydrophobicity of coating materials. Thus, the incorporation of silica into the epoxy matrix at the molecular level does indeed change the surface characteristics of the hybrid sol-gel materials significantly. The as-prepared hybrid sol-gel materials incorporation of silica were found to exhibit much hydrophobic characteristics relative to the pure epoxy. This increased hydrophobic property might also lead the as-prepared hybrid sol-gel materials to

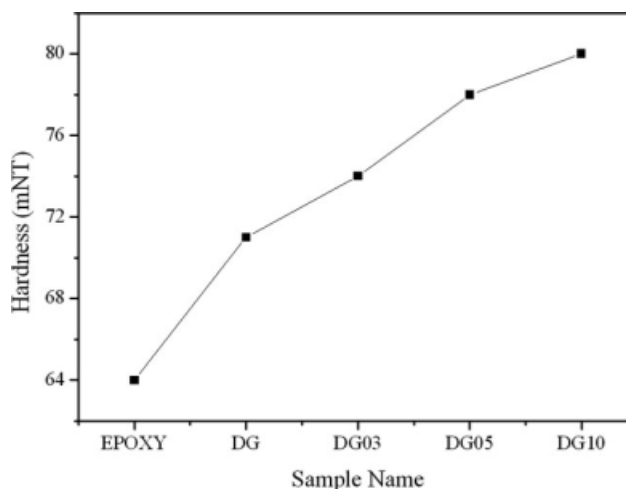


Figure 8 The hardness test of epoxy and epoxy-silica hybrid sol-gel materials measured by Shore D.

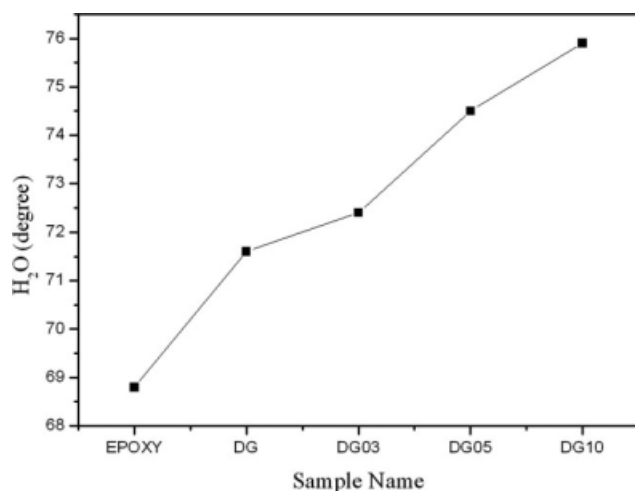


Figure 9 Contact angles of water on the surface of epoxy and epoxy-silica hybrid sol-gel coatings at various silica contents.

be potentially used in the application of corrosion protection coatings.

SEM cross-section

SEM was used to investigate the morphology of neat epoxy [shown in Fig. 10(a)] and epoxy-silica hybrid materials [shown in Fig. 10(b,c)]. SEM micrograph of fractured surface of the epoxy material reveals a smooth, glassy, and homogeneous microstructure without any plastic deformation. Whereas, the fractured surfaces of the epoxy-silica hybrid materials show the presence of heterogenous morphology and the heterogeneity increases with increasing siloxane content (5–10%). This observation also confirms the existence of inter-crosslinking network structure in epoxy-silica hybrid materials to enhance the mechanical properties.

Surface morphology

To further gain the physical fundamentals of the topographical structures in detail, an AFM was applied to investigate the surface profiles of the samples. The surface morphology of the hybrid sol-gel coating was investigated by AFM using a contact mode. As shown in Figure 11, according to the 3D image analysis, it demonstrated a slightly smooth increase of topography as the polymer epoxy matrix incorporated with 5 wt % loading of inorganic silica. The average roughness (R_a) and root mean square roughness (R_q) of the sample epoxy, DG and DG05 were summarized in Table II, suggesting that the hybrid sol-gel materials might have no organic-inorganic phase separation, indicating that the SiO₂ particles were well dispersed in the epoxy matrix as shown in the TEM micrograph (Fig. 3). It exhibited

good compatibility with the epoxy matrix for SiO₂ with 3-glycidoxypropyl-trimethoxysilane coupling agent. Therefore, the incorporation of low silica content into the polymer matrix may effectively enhance the flatness.^{33,34}

CONCLUSION

In this article, a series of sol-gel hybrid materials consisted of epoxy and inorganic silica were successfully prepared. Subsequently, the epoxy-silica hybrid

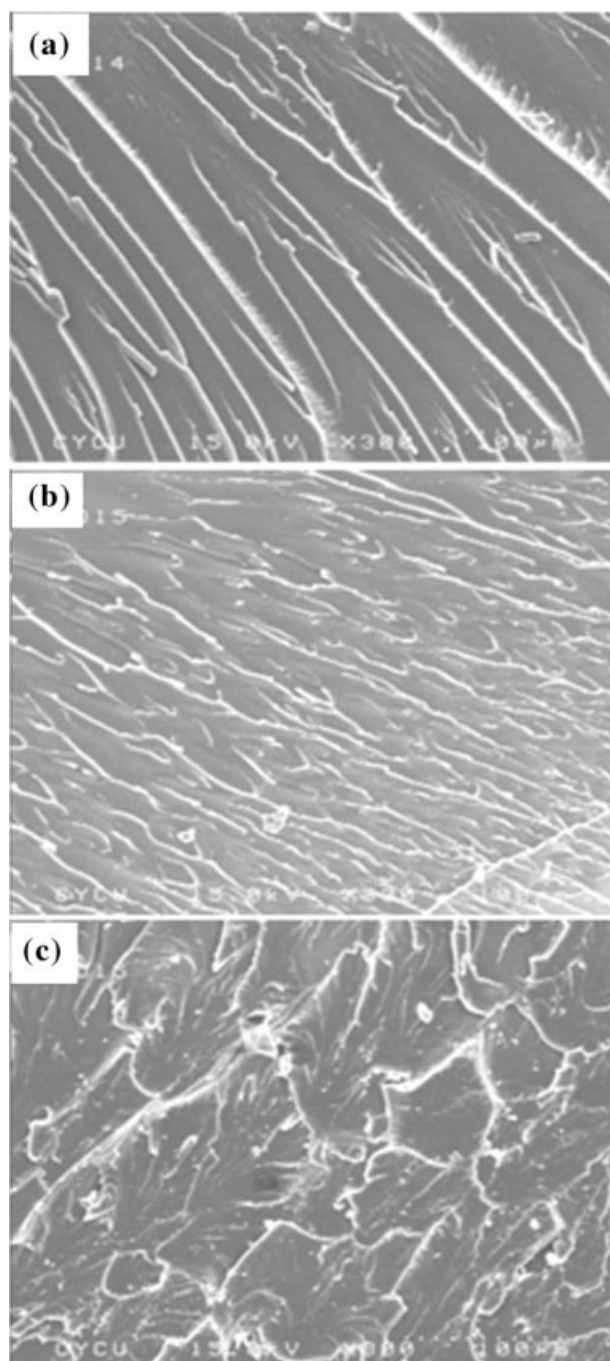


Figure 10 SEM micrographs of the fracture surfaces of (a) epoxy, (b) DG05, and (c) DG10 ($\times 300$).

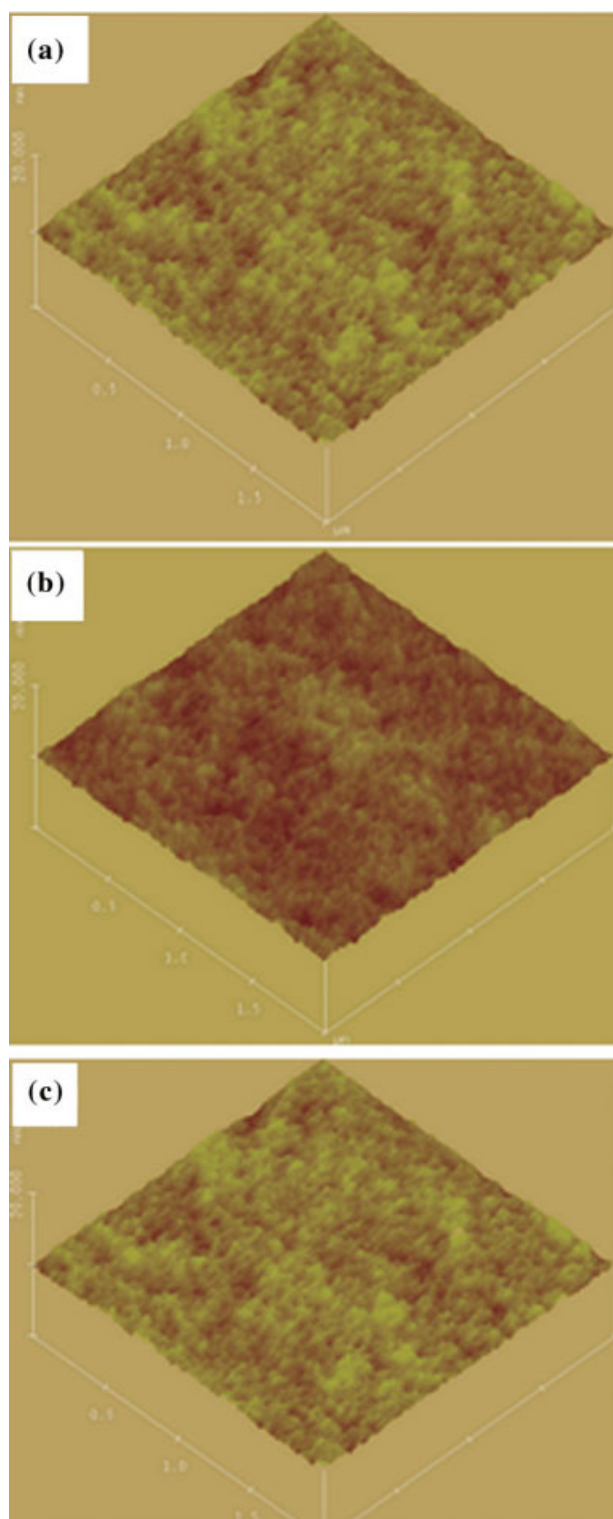


Figure 11 AFM surface images ($1 \times 1 \mu\text{m}^2$) of (a) epoxy, (b) DG, and (c) DG05. [Color figure can be viewed in the online issue, which is available at www.interscience.wiley.com.]

sol-gel materials were prepared by HCl-catalyzed hydrolysis/polycondensation reactions of sol-gel precursors and TMOS simultaneously.

The hybrid sol-gel coatings in the form of coating were found to show advanced corrosion protection effect on CRS coupons relative to the pure epoxy based on the electrochemical measurement of corrosion potential, polarization resistance, and corrosion current. The increase of adhesion strength of hybrid coatings (e.g., DG10) on CRS coupons may be attributed to the formation of Fe—O—Si covalent bond at the interface of coatings/CRS system based on the curve fitting of FTIR-RAS spectrum studies. For example, compared with pure epoxy, the curve fitting spectrum of FTIR-RAS studies for the as-prepared hybrid coating DG10 showing two novel peaks. The band at 995 cm^{-1} corresponded to Fe—O—Si, which indicated that the covalent bond was made between CRS and hybrid sol-gel coating on the CRS surface.

The SiO_2 nanoparticles which are well dispersive in hybrid materials by sol-gel technology were found to lead more effectively enhanced on the thermal stability, mechanical strength of as-prepared hybrid epoxy-silica sol-gel materials in the form of bulky materials were investigated by TGA, DSC, DMA, hardness meter, and SEM, respectively. The water contact angle increased with the increase in silica content in the hybrid sol-gel coatings, reflecting to an increase in hydrophobicity of coating materials. The surface roughness of hybrid sol-gel coatings decreased as the amount of silica was increased based on the AFM.

References

- Uhlig, H. H. *Corrosion and Corrosion Control*; Wiley: New York, 1971.
- Basic, J. M. *Corrosion and Oxidation*; Halsted Press: New York, 1980.
- Jang, J.; Kim, E. K. *J Appl Polym Sci* 1995, 71, 585.
- Schrader, M. E.; Cardomone, J. A. *J Adhes* 1978, 9, 305.
- Boerio, F. J.; Dillingham, R. G.; Snow, A. R. *Org Coat Plast Chem Prep* 1984, 50, 444.
- Kaul, A.; Sung, N. H.; Chin, I.; Sung, C. S. P. *Polym Eng Sci* 1984, 24, 493.
- Thiedman, W.; Tolan, F. C.; Pearce, P. J.; Morris, C. E. M. *J Adhes* 1987, 22, 197.
- Pluedemann, E. P. *Silane Coupling Agents*, 2nd ed.; Plenum Press: New York, 1990.
- Kato, K. *J Mater Sci* 1992, 27, 1445.
- Kato, K. *J Mater Sci* 1993, 28, 4033.
- Holmes-Farley, S. D.; Yanyo, L. C. *J Adhes Sci Technol* 1991, 5, 131.
- Frings, S.; Meinema, H. A.; Van Nostrum, C. F.; Vander-Linde, R. *Prog Org Coat* 1998, 33, 126.
- Messadeq, S. H.; Pulcinelli, S. H.; Santilli, C. V.; Guastaldi, A. C.; Messadeq, Y. *J Non-Cryst Solids* 1999, 247, 164.
- Tuman, S. J.; Soucek, M. D. *J Coat Technol* 1996, 68, 854.
- Berger, D. M. *Met Finish* 1975, 73, 46.
- Holmes-Farley, S. R.; Yanyo, L. C. *Mater Res Soc Symp Proc* 1990, 180, 439.
- Tan, N. C. B.; Bauer, B. J.; Plestil, J.; Barnes, J. D.; Liu, D.; Matejka, L.; Dusek, K.; Wu, W. L. *Polymer* 1999, 40, 4603.

18. Matejka, L.; Plestil, J.; Dusek, K. *J Non-Cryst Solids* 1998, 226, 114.
19. Mascia, L.; Tang, T. *J Sol-Gel Sci Technol* 1998, 13, 405.
20. Nishilima, S.; Hussain, M.; Nakahira, A. *Mater Res Soc Symp Proc* 1996, 435, 369.
21. Yeh, J. M.; Huang, H. Y.; Cheng, C. L.; Su, W. F.; Yu, Y. H. *Surf Coat Technol* 2006, 200, 2753.
22. Yeh, J. M.; Weng, C. J.; Liao, W. J.; Mau, Y. W. *Surf Coat Technol* 2006, 201, 1788.
23. Yeh, J. M.; Liou, S. J.; Lai, C. Y.; Wu, P. C. *Chem Mater* 2001, 13, 1131.
24. Yeh, J. M.; Chen, C. L.; Chen, Y. C.; Ma, C. Y.; Lee, K. R.; Wei, Y.; Li, S. *Polymer* 2002, 43, 2729.
25. Yu, Y. H.; Yeh, J. M.; Liou, S. J.; Chang, Y. P. *Acta Mater* 2004, 52, 475.
26. Ananda Kumar, S.; Sankara Narayanan, T. S. N. *Prog Org Coat* 2002, 45, 323.
27. Liu, Y. L.; Lin, Y. L.; Chen, C. P.; Jeng, R. J. *J Appl Polym Sci* 2003, 90, 4047.
28. Ochi, M.; Takahashi, R. *J Appl Polym Sci Part B: Polym Phys* 2001, 39, 1071.
29. Chiang, C. L.; Ma, C. C. M. *Eur Polym J* 2002, 38, 2219.
30. Stern, M.; Geary, A. L. *J Electrochem Soc* 1957, 104, 56.
31. Bockris, J.; Reddy, K. N. *Modern Electrochemistry*; Wiley: New York, 1976; p 622.
32. Kong, X.; Narine, S. S. *Biomacromolecules* 2008, 9, 1424.
33. Yeh, J. M.; Weng, C. J.; Huang, K. Y.; Huang, H. Y.; Yu, Y. H.; Yin, C. H. *J Appl Polym Sci* 2003, 88, 1072.
34. Wei, Y.; Jin, D.; Brennan, D. J.; Rivera, D. N.; Zhuang, Q.; DiNardo, N. J.; Qiu, K. *Chem Mater* 1998, 10, 769.